``Enseigner la recherche en train de se faire''

Chaire de
Physique de la Matière Condensée

PETITS SYSTEMES THERMOELECTRIQUES: *CONDUCTEURS MESOSCOPIQUES ET GAZ D'ATOMES FROIDS*

Cycle « Thermoélectricité »
2012 - 2014

Antoine Georges

Séance du 19 novembre 2013
Cours 3

Energy Filtering and Thermoelectric Efficiency

Cours 4: Thermal Transport in the Quantum Regime.

Séminaire :

Olivier Bourgeois (Institut Néel, Grenoble)

Nanophononique : du transport de phonons à basse température aux applications en thermoélectricité

Reconsidering the entropy current…

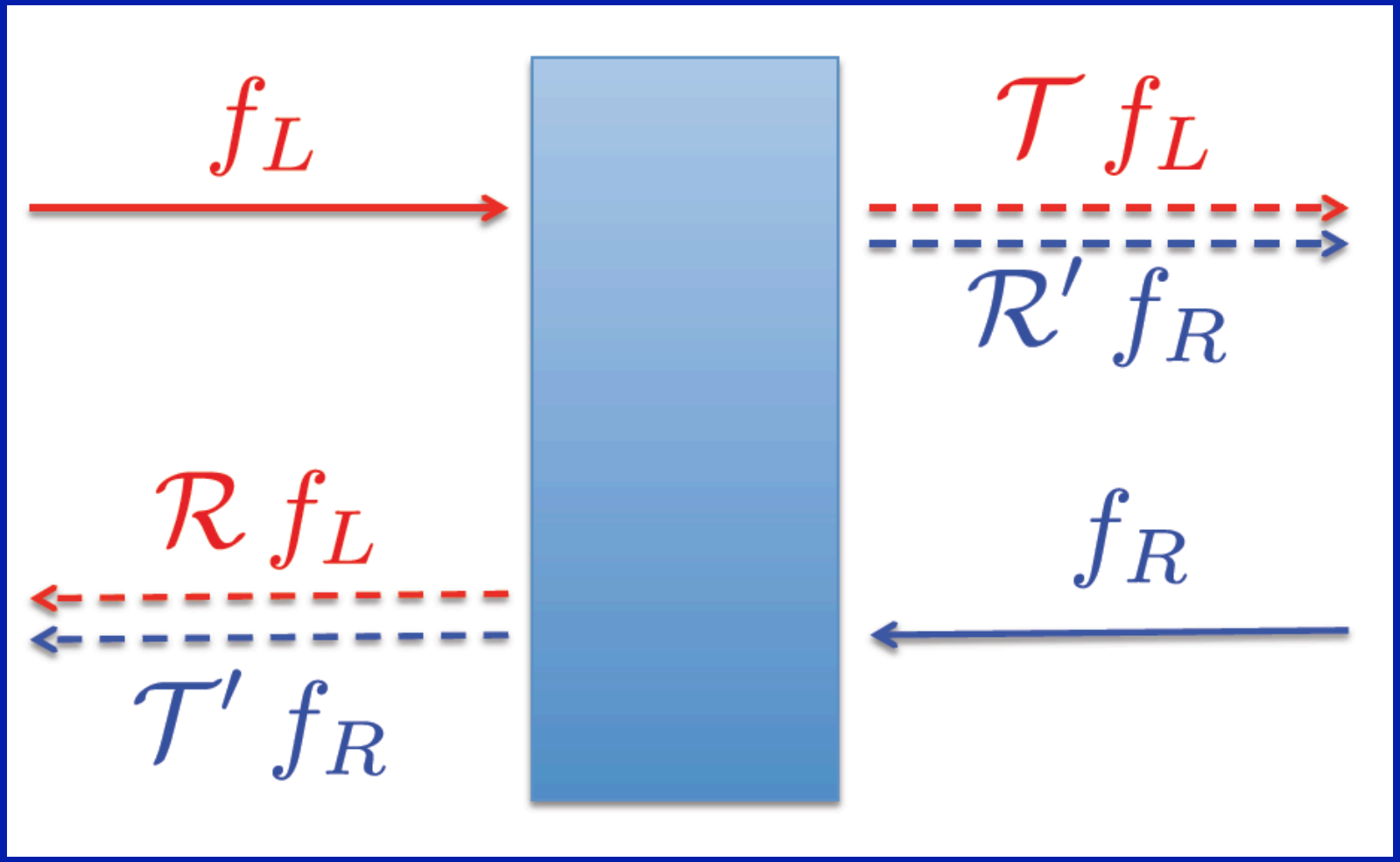

Improving thermoelectric efficiency by ‘energy filtering’

Engineering
the energy-dependence of the
- Transport function
- Density of states
- Transmission coefficient etc…

Two key articles…

PHYSICAL REVIEW B VOLUME 47, NUMBER 19 15 MAY 1993-I

Effect of quantum-well structures on the thermoelectric figure of merit

L. D. Hicks
Department of Physics, Massachusetts Institute of Technology, Cambridge, Massachusetts 02139

M. S. Dresselhaus
Department of Electrical Engineering and Computer Science and Department of Physics, Massachusetts Institute of Technology, Cambridge, Massachusetts 02139
(Received 3 December 1992)

Mildred Dresselhaus, MIT

Also: PRB 47, 16631 (1993) > 2000 citations for the 2 papers

Originally envisioned as improvement of electronic properties, but turned out to be also/especially efficient for lowering thermal conductivity !

Reports of ZT > 2

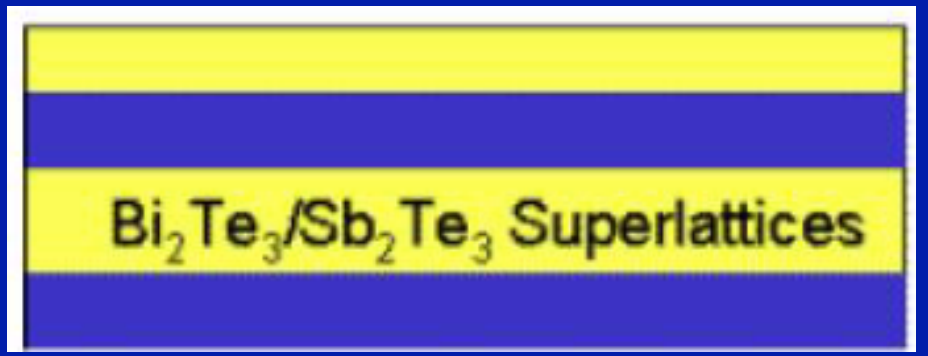

Proc. Natl. Acad. Sci. USA
Vol. 93, pp. 7436–7439, July 1996
Applied Physical Sciences

This contribution is part of a special series of Inaugural Articles by members of the National Academy of Sciences elected on April 25, 1995.

The best thermoelectric

G. D. MAHAN*† AND J. O. SOFO‡

*Department of Physics and Astronomy, The University of Tennessee, Knoxville, TN 37996-1200; †Solid State Division, Oak Ridge National Laboratory, P.O. Box 2008, Oak Ridge, TN 37831-6030; and ‡Instituto Balseiro, Centro Atomico Bariloche, (8400) Bariloche, Argentina

Contributed by G. D. Mahan, May 20, 1996

ABSTRACT **What electronic structure provides the largest figure of merit for thermoelectric materials? To answer that question, we write the electrical conductivity, thermopower, and thermal conductivity as integrals of a single function, the transport distribution. Then we derive the mathematical function for the transport distribution, which gives the largest figure of merit. A delta-shaped transport distribution is found to maximize the thermoelectric properties. This result indicates that a narrow distribution of the energy of the electrons participating in the transport process is needed for maximum thermoelectric efficiency. Some possible realizations of this idea are discussed.**

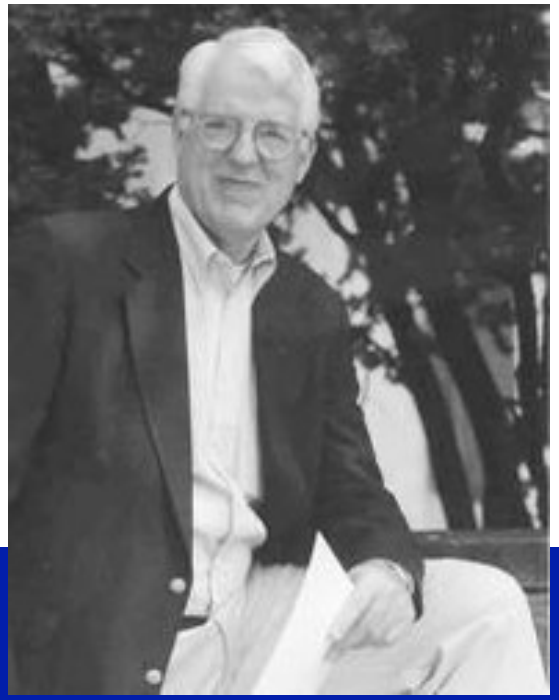

Nature Nanotechnologies 8, 471 (2013)

commentary

When thermoelectrics reached the nanoscale

Joseph P. Heremans, Mildred S. Dresselhaus, Lon E. Bell and Donald T. Morelli

The theoretical work done by Lyndon Hicks and Mildred Dresselhaus 20 years ago on the effect of reduced dimensionality on thermoelectric efficiency has had deep implications beyond the initial expectations.

In the early 1990s, Mildred Dresselhaus was asked by the US Navy, in conjunction with a request from the French Navy (by John Stockholm and Michel Bénicourt, Ingénieur Général de l'Armement) to suggest ideas for increasing ZT in thermoelectric materials. Dresselhaus suggested a new concept: to use low dimensionality for increasing $\alpha^2 n$ and for decreasing κ_φ. In

Dimensionless figure of merit *vs.* time

Heremans et al.
Nature Nanotechnologies 8, 471 (2013)

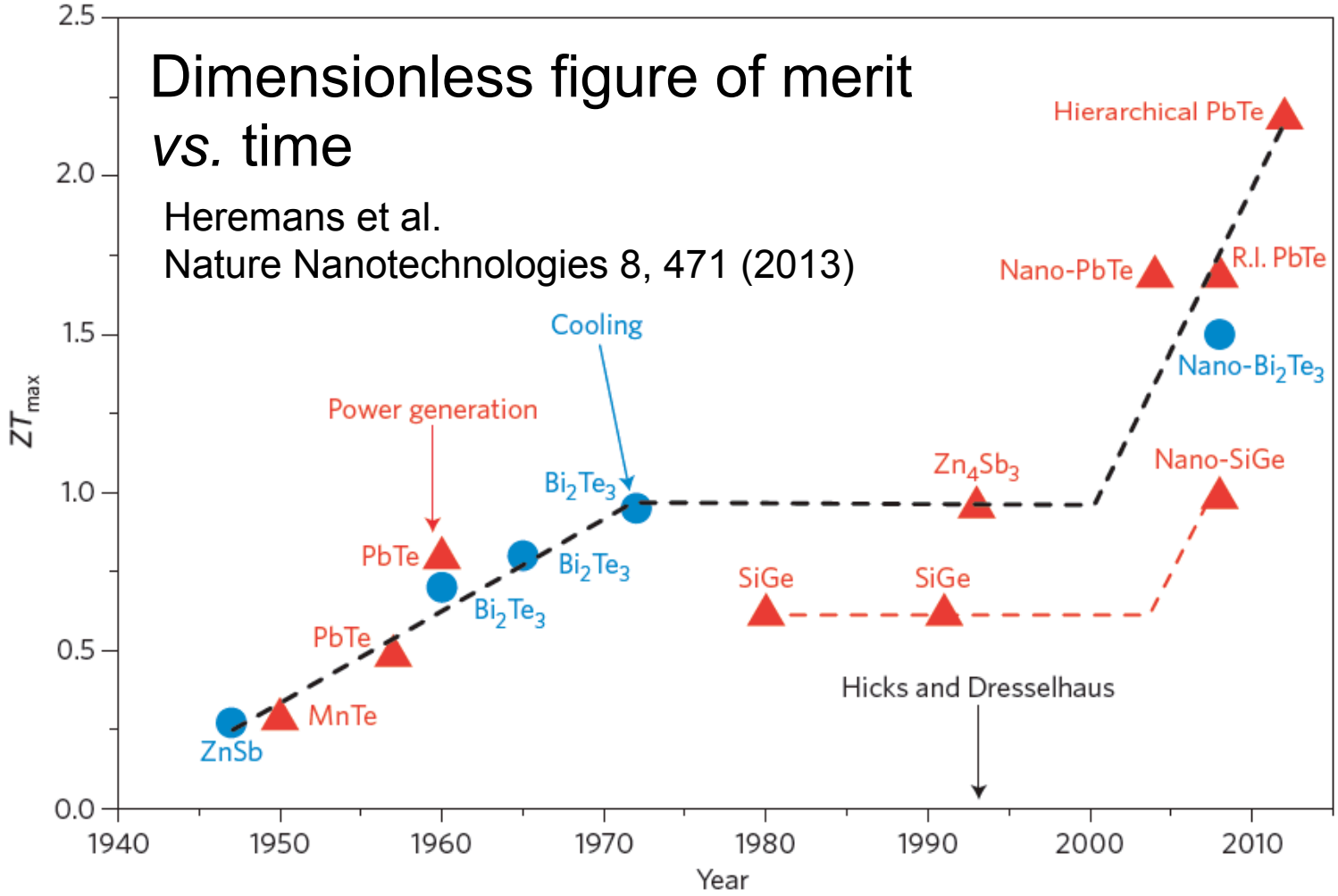

Figure 1 | Evolution of the maximum *ZT* over time. Materials for thermoelectric cooling are shown as blue dots and for thermoelectric power generation as red triangles. The black dashed line guides the eye. The compound semiconductors (PbTe, Bi_2Te_3) indicate only the basic constituent; most high *ZT* materials are alloys or nanocomposites. No data are shown for skutterudites (which can achieve *ZT*~1.7 in n-type materials) because they do not benefit from nanostructuring. References for the *ZT* of nanoscale thermoelectric materials are: nano-SiGe (ref. 31), nano-PbTe (a PbTe–$AgTeSb_2$ nanocomposite; ref. 25), R. I. PbTe (PbTe doped with the resonant impurity (R. I.) Tl; ref. 12), nano-Bi_2Te_3 (ref. 30) and hierarchical PbTe (ref. 32).

Number of articles on Thermoelectrics:

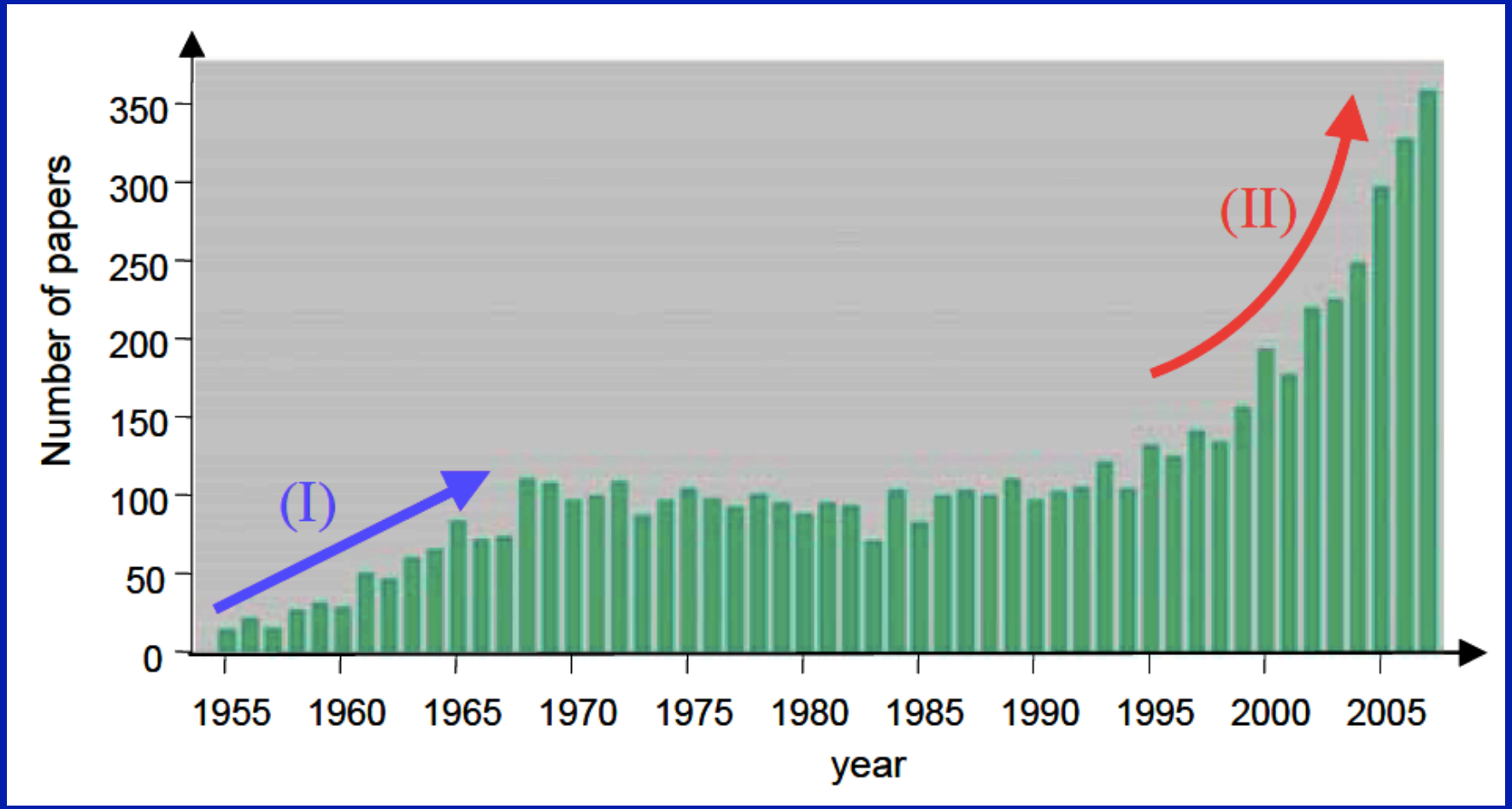

JC Zheng
Front. Phys. China
3 (2008) 269

Data obtained from database of "ISI Web of Knowledge" with search option of "thermoelectric or thermoelectrics" in Title only. http://www.isiwebofknowledge.com/ (accessed March 19, 2008).

Reminders on Thermoelectric Efficiency

For details and derivations, see spring 2013 lectures and notes

In generator mode:

- Power delivered: $I\Delta V = I_N \Delta\mu$
- Heat provided by (left) hot source: $T_L I_S$

Efficiency $$\eta = -\frac{I_N \, \Delta\mu}{I_S \, T_L} = \eta_c \, \eta_r$$

Carnot efficiency $$\eta_c = 1 - \frac{T_R}{T_L} = \frac{\Delta T}{T_L}$$

Efficiency relative to Carnot $$\boxed{\eta_r = -\frac{I_N \, \Delta\mu}{I_S \, \Delta T}}$$

Irreversibly dissipated heat in linear response:

$$\frac{\partial Q}{\partial t}|_{irr} = T\frac{\partial S}{\partial t}|_{irr} = I_N \Delta\mu + I_S \Delta T$$

$$= I\Delta V + I_Q \frac{\Delta T}{T}$$

→ 0 for Carnot (reversible) process with $\eta_r = 1$

Optimization variable: ratio of the tension to the `stopping' tension (given by Seebeck condition I_N=0):

$$\xi \equiv \frac{\Delta\mu}{\Delta\mu_{stop}} = -\frac{L_{11}}{L_{12}}\frac{\Delta\mu}{\Delta T} = \frac{\Delta V}{\alpha\Delta T}$$

Expressing the ratio: $\frac{I_N}{I_S} = \frac{L_{11}\Delta\mu + L_{12}\Delta T}{L_{21}\Delta\mu + L_{22}\Delta T}$ we obtain:

Efficiency relative to Carnot:

$$\boxed{\eta_r = \frac{\xi(1-\xi)}{1/g^2 - \xi}}$$

Where the dimensionless coupling constant is:

$$\boxed{g^2 \equiv = \frac{L_{12}L_{21}}{L_{11}L_{22}} = \frac{L_{12}^2}{L_{11}L_{22}} \in [0,1]}$$

Relation to ``dimensionless figure of merit'':

$$\overline{Z} \equiv ZT \equiv \frac{\alpha^2 G}{G_{th}/T} = \frac{g^2}{1-g^2}$$

$$g^2 = \frac{\overline{Z}}{1+\overline{Z}}$$

Power: $$P = \frac{1}{4}(\Delta T)^2 \left[\alpha^2 G\right] \xi(1-\xi)$$ $\alpha^2 G$: `power factor'

Maximum POWER is for ξ=1/2 (half the stopping force)
Maximum EFFICIENCY is for $\xi^\star = (1-\sqrt{1-g^2})/g^2$

$$\eta_r^{max} = \frac{\sqrt{\overline{Z}+1}-1}{\sqrt{\overline{Z}+1}+1} = \frac{1-\sqrt{1-g^2}}{1+\sqrt{1+g^2}}$$

Maximum efficiency
→ 1 for g→1 (Carnot), P=0 !

$$\eta_r(P_{max}) = \frac{\overline{Z}}{2(2+\overline{Z})} = \frac{g^2}{2(2-g^2)}$$

Efficiency at Max. Power
→ 1/2 for g→1
(Chambadal-Novikov-CA)

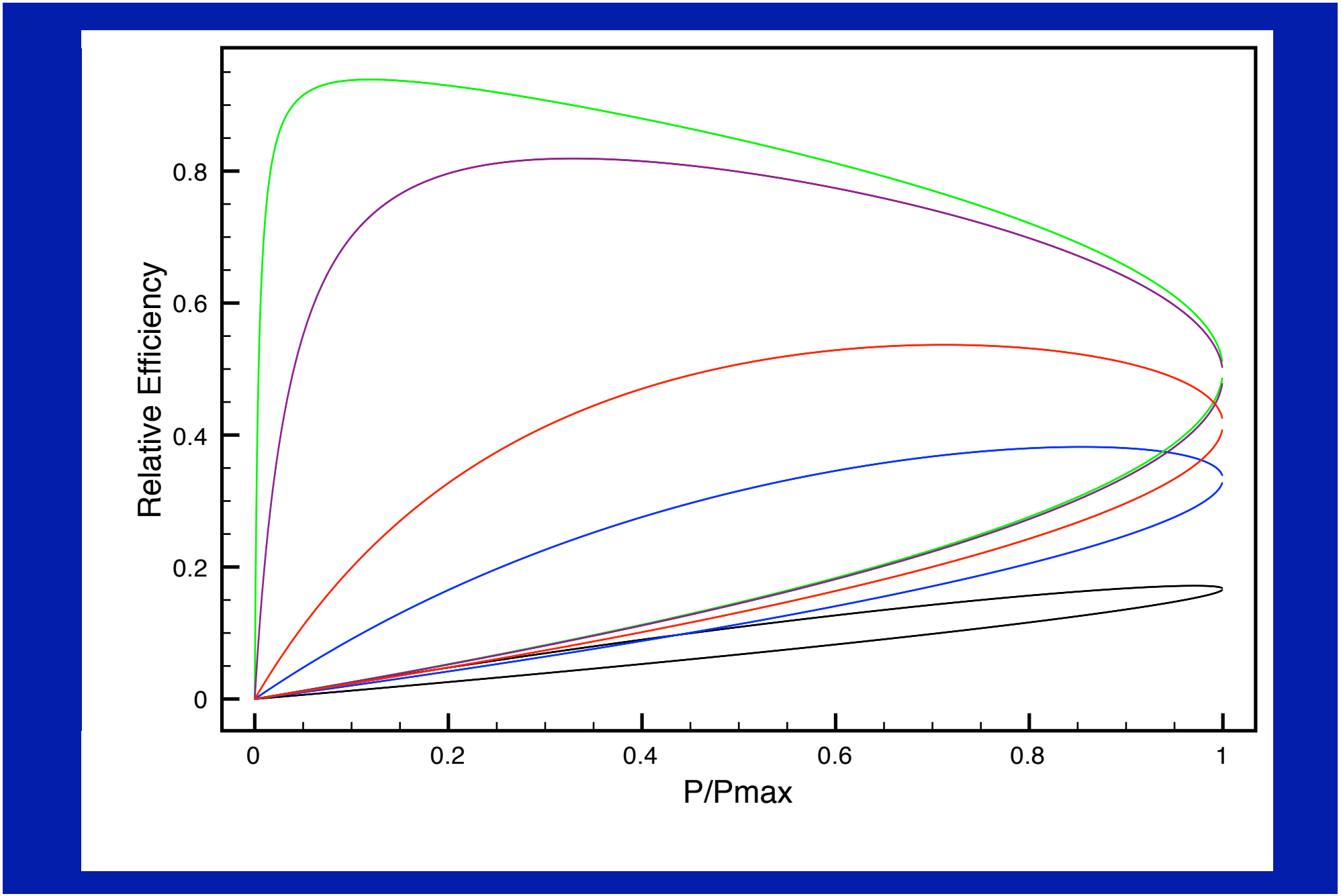

FIG. 4: Relative efficiency vs. power normalized to its maximum value, for (bottom to top): $\overline{z} = 1, 4, 10, 100, 1000$. The upper (resp. lower) branches correspond to a force ratio $x \geq 1/2$ (resp. $x \leq 1/2$). Maximum efficiency is realized on the upper branch.

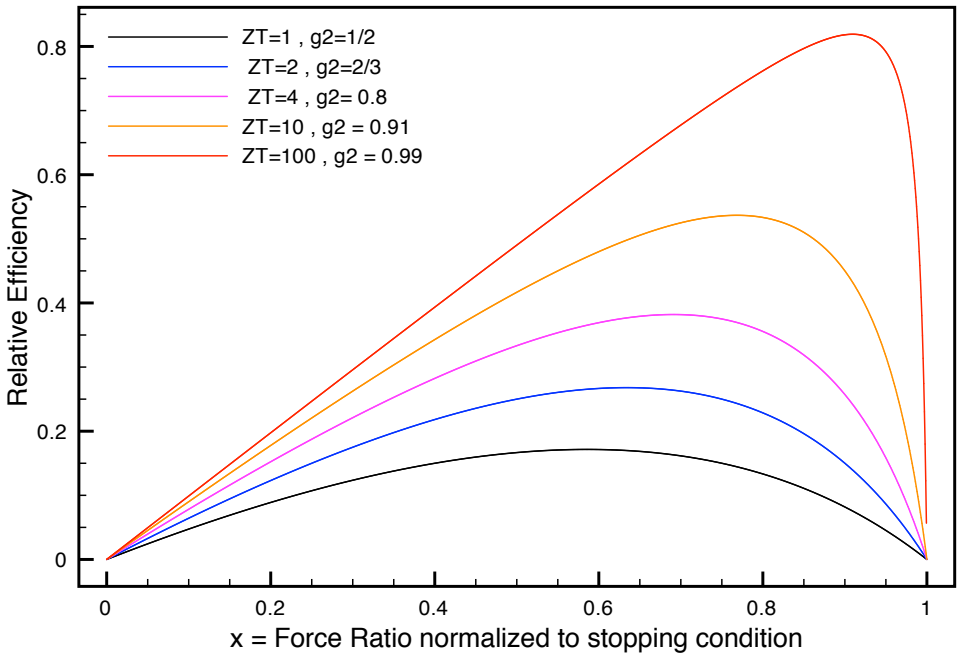
ZT=1 , g2=1/2
ZT=2 , g2=2/3
ZT=4 , g2= 0.8
ZT=10 , g2 = 0.91
ZT=100 , g2 = 0.99
Relative Efficiency
0
0.2
0.4
0.6
0.8
1
x = Force Ratio normalized to stopping condition

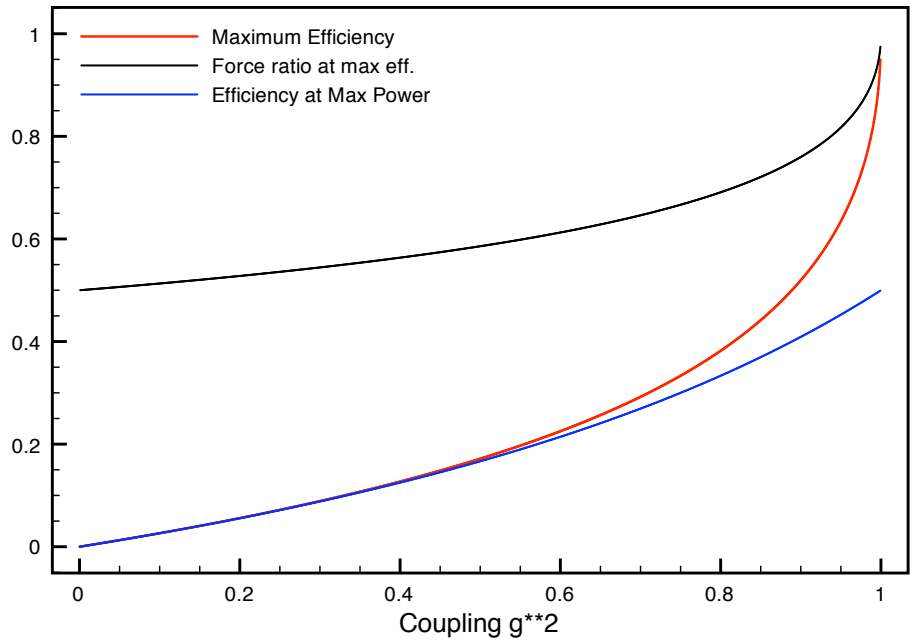
Maximum Efficiency
Force ratio at max eff.
Efficiency at Max Power
0
0.2
0.4
0.6
0.8
1
Coupling g**2

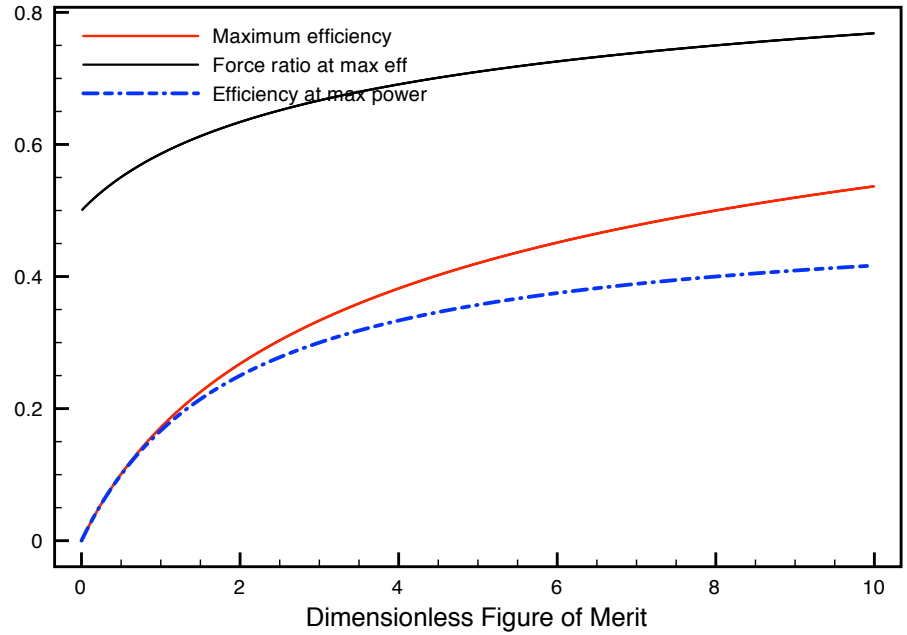
Maximum efficiency
Force ratio at max eff
Efficiency at max power
0
0.2
0.4
0.6
0.8
0
2
4
6
8
10
Dimensionless Figure of Merit

Note: All this is done within linear response
A number of recent works
consider the efficiency
beyond linear response

- See for examples, for references:
- G. Casati et al. arXiv:1311.4430 (review)
- R.S.Whitney arXiv:1306.0826

Reminders from lecture 2: Conductance, Thermopower, and Thermal Conductance:

$$L_{11} = \frac{2}{h} I_0$$

$$L_{12} = \frac{2}{h} k_B \, I_1$$

$$L_{22} = \frac{2}{h} k_B^2 \, I_2$$

$$G = \frac{2e^2}{h} I_0 \quad , \quad \left(\frac{h}{e^2} = 25.81 k\Omega \right)$$

$$\alpha = -\frac{k_B}{e} \frac{I_1}{I_0} \quad , \quad \left(\frac{k_B}{e} = 86.3 \, \mu V K^{-1} \right)$$

$$\frac{G_{th}}{T} = \frac{2}{h} k_B^2 \left[I_2 - \frac{I_1^2}{I_0} \right]$$

$$\mathcal{L} \equiv \frac{G_{th}}{TG} = \left(\frac{k_B}{e} \right)^2 \left[\frac{I_2}{I_0} - \left(\frac{I_1}{I_0} \right)^2 \right]$$

Dimensionless integrals:

$$I_n \equiv \int d\varepsilon \, \mathcal{T}(\varepsilon) \left(\frac{\varepsilon - \mu}{k_B T} \right)^n \left(-\frac{\partial f}{\partial \varepsilon} \right)$$

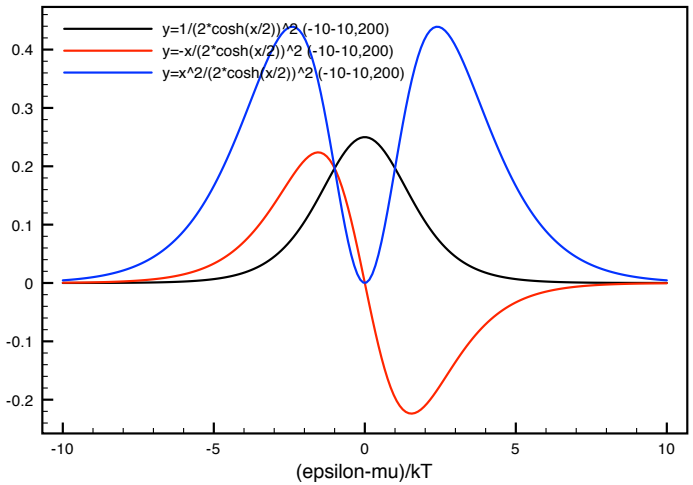

Bulk Materials:

Same expressions apply for conductivity (electrical and thermal) and thermopower, with T(ε) now the transport function:

$$\mathcal{T}(\varepsilon) \sim \sum_{\mathbf{k}} \tau_{\mathbf{k}} v_{\mathbf{k}}^2 \delta(\varepsilon - \varepsilon_{\mathbf{k}})$$

From Boltzmann equation, *see spring 2013 lectures*

A useful observation

cf. Mahan and Sofo, PNAS 93, 7436 (1996)

Think of:

$$p(\varepsilon) \equiv \frac{\mathcal{T}(\varepsilon)[-f'(\varepsilon)]}{\int d\varepsilon \mathcal{T}(\varepsilon)[-f'(\varepsilon)]} = \frac{g(\epsilon)}{G}$$

As a probability density, measuring the contribution to the total conductance of states around a given energy (for a given gate voltage)

Or even better:

$$x \equiv \frac{\varepsilon - \mu}{k_B T} \;,\; p(x) \equiv \frac{\mathcal{T}(\mu + k_B T\, x)}{4G \cosh^2 \frac{x}{2}} \;,\; \int dx\, p(x) = 1$$

Transmission coefficient (transport function) leading to $g^2 \rightarrow 1$ (Mahan-Sofo) :

$$g^2 = \frac{I_1^2}{I_0 I_2} = \frac{\langle (\varepsilon - \mu) \rangle_p^2}{\langle (\varepsilon - \mu)^2 \rangle_p} = \frac{\langle x \rangle_p^2}{\langle x^2 \rangle_p}$$

Clearly, a narrow transport function (transmission coefficient)
- approaching asymptotically a δ-function -
brings g close to unity

Note however:
This may not yield the best output power, since the power factor is ~ I_1^2/I_0

Ilustrate this for a single resonant level
In the context of mesoscopics:
- Quantum Dots -

Early theory work: Beenakker and Staring PRB 46, 9667 (1992)
Experimental: Molenkamp et al., see seminar 12/11/2013
Efficiency: Nakpathomkun et al. PRB 82, 235428 (2010)
(see also: Mani et al. J. Elec. Mat 38, 1163 (2009)

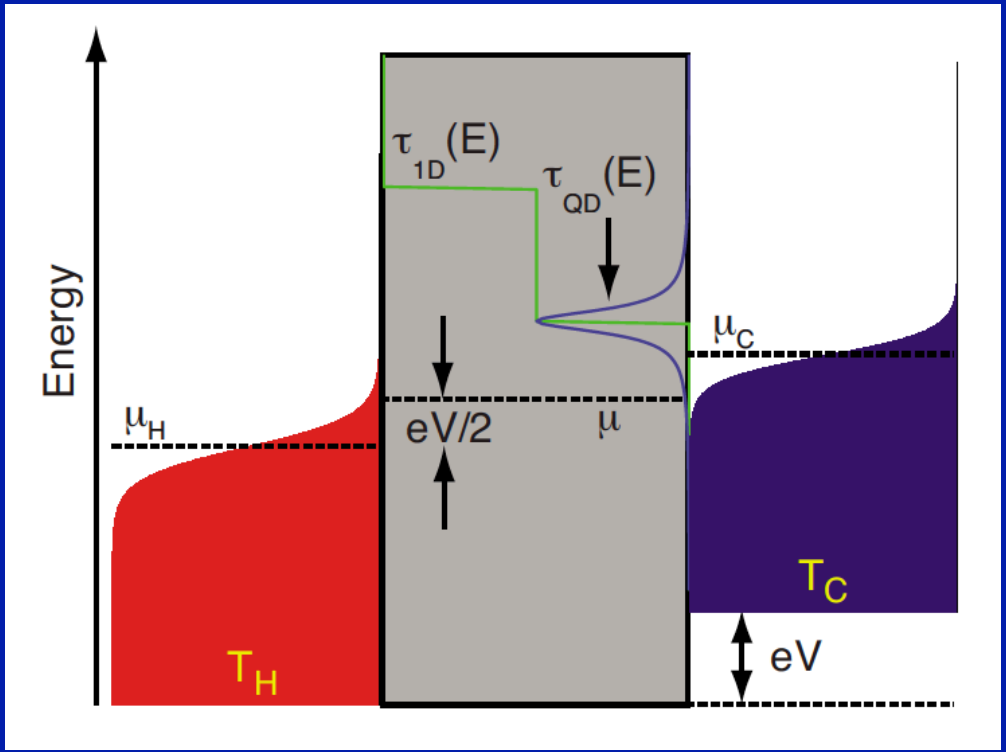

Nakpathomkun et al.

Transmission coefficient is a Lorentzian:

$$\mathcal{T}(\varepsilon) = \frac{\Gamma_R \Gamma_L}{(\varepsilon - \varepsilon_r)^2 + (\Gamma_L + \Gamma_R)^2/4}$$

$$= \frac{(\Gamma/2)^2}{(\varepsilon - \varepsilon_r)^2 + (\Gamma/2)^2} \quad (\Gamma_R = \Gamma_L = \frac{\Gamma}{2})$$

Two control parameters: $\dfrac{\mu - \varepsilon_r}{k_B T}$, $\dfrac{\Gamma}{k_B T}$

$$I_n = \int dx \frac{x^n}{4\cosh^2 x/2} \frac{(\Gamma/2k_B T)^2}{\left(\frac{\mu-\varepsilon_r}{k_B T} + x\right)^2 + (\Gamma/2k_B T)^2}$$

Coupling constant $g^2 \left[\dfrac{\mu - \varepsilon_r}{k_B T}, \dfrac{\Gamma}{k_B T}\right]$

For fixed Γ/kT optimize over bias Δμ AND μ-ε_r

Nakpathomkun et al.
PRB 82, 235428 (2010)

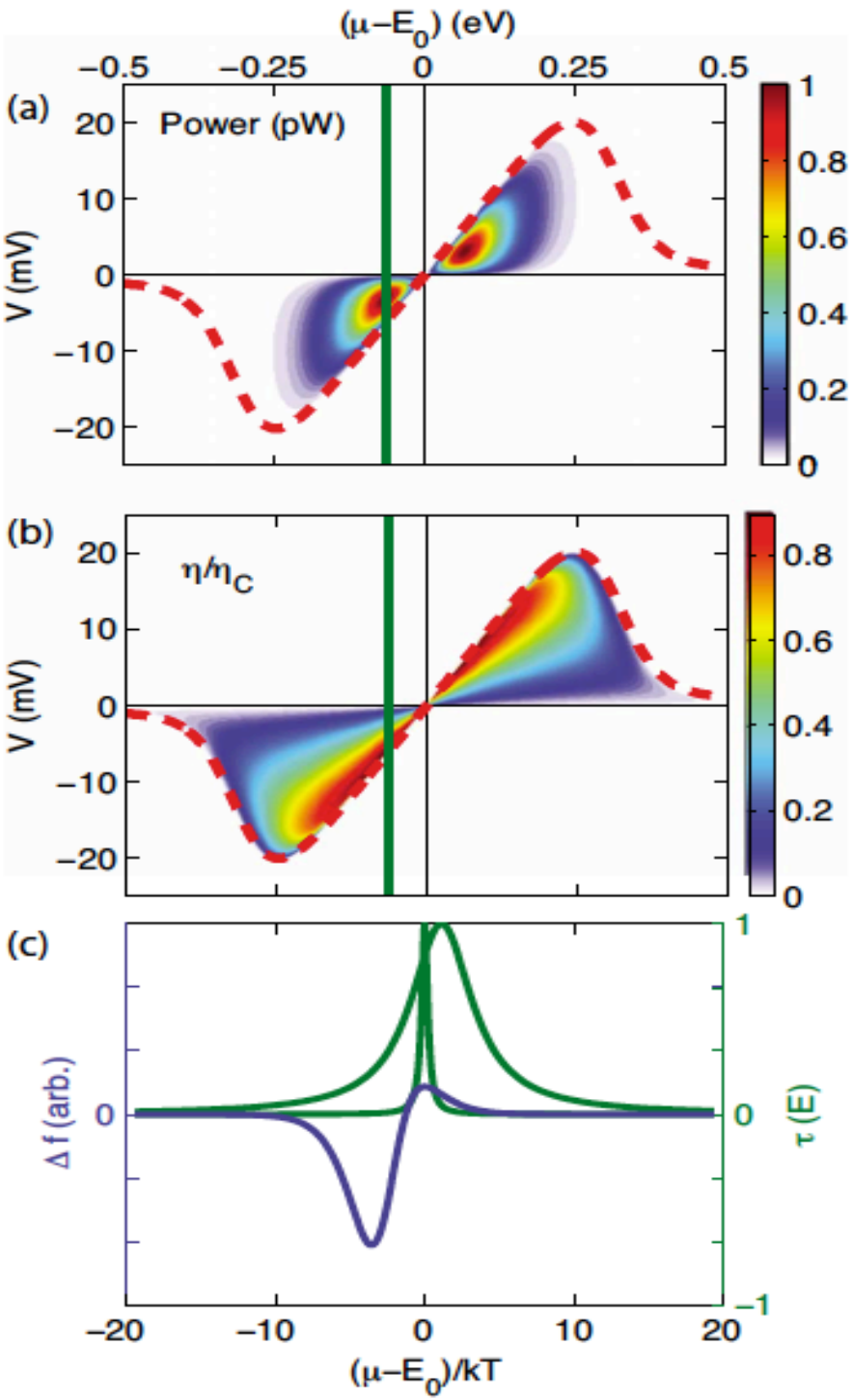

FIG. 2. (Color online) (a) Power and (b) efficiency normalized by Carnot efficiency, of a QD as a function of bias voltage V and average chemical potential μ, for T_C=300 K, T_H=330 K ($\Delta T/T_C$=0.1), and Γ=0.01kT. The open-circuit voltage, V_{oc} is highlighted in (red) dashed line (peak V_{oc} corresponds to $S \approx 2$ meV/K). The system works as a generator when the bias is between zero and V_{oc}. The vertical green line indicates the μ where maximum power occurs. (c) Current through a QD is the integral over the product of τ_{QD} (green) [Eq. (3)] and $\Delta f=(f_H-f_C)$, shown here in blue, using the μ and V that result in P_{max}. Two transmission widths, Γ=0.5kT and 5kT are plotted here in the approximate position where maximum power would be achieved.

Max efficiency, Max Power, Efficiency at Max Power vs. Γ/kT

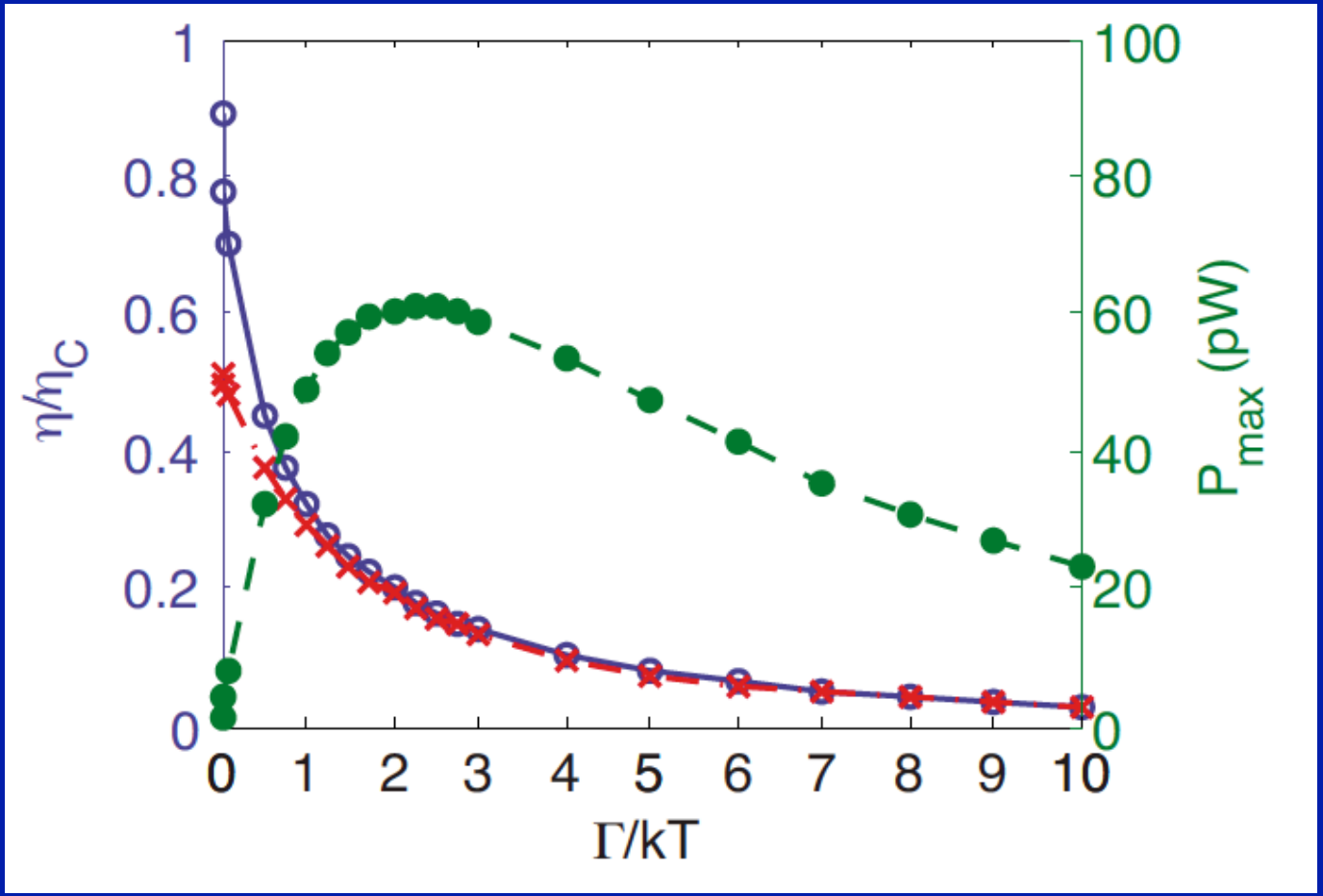

Efficiency is harmed by tails of the Lorentzian distribution causing too energetic electrons to waste heat in energy production and other electrons to travel in the wrong direction

Low-T limit kT<<Γ: Sommerfeld expansion as above

$$G = \frac{2e^2}{h}\mathcal{T}(\mu) = \frac{2e^2}{h}\frac{(\Gamma/2)^2}{(\mu-\varepsilon_r)^2+(\Gamma/2)^2}$$

$$\alpha \simeq -\frac{k_B}{e}\frac{\pi^2}{3}k_BT\frac{\partial}{\partial\mu}\ln\mathcal{T}(\mu)$$

$$= \frac{2\pi^2}{3}\frac{k_B}{e}\frac{(\mu-\varepsilon_r)/k_BT}{[(\mu-\varepsilon_r)/k_BT]^2+(\Gamma/2k_BT)^2}$$

Hi-T limit Γ<<kT<<ΔE: Universal limit (Mani et al.)

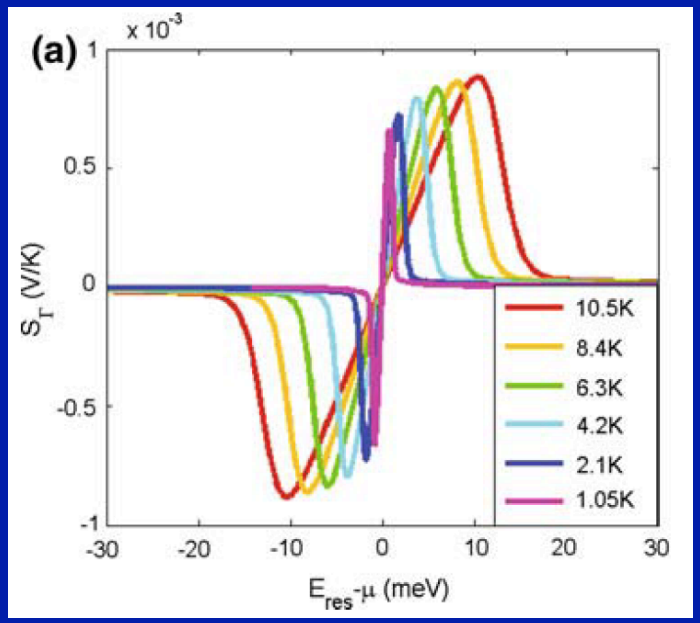

$$\alpha = -\frac{k_B}{e}\frac{\varepsilon_r-\mu}{k_BT}$$

`sawtooth'

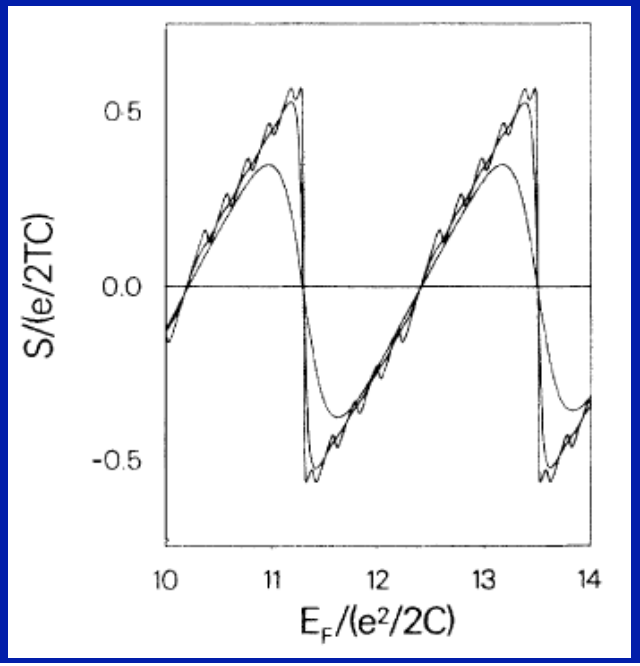

Reversible heat engines with resonant tunneling: qualitative picture

(realized in a quantum dot for Γ >>kT)

Humphrey et al. PRL 89 116801 (2002)

In this (Mahan-Sofo) limit, g→1 and:

$$\eta_r = \xi = \frac{\Delta\mu}{\Delta\mu_{stop}} = \frac{T}{\Delta T}\frac{\Delta\mu}{\mu - \varepsilon_r}$$

Carnot efficiency applies when the level position is chosen such that 'stopping condition' is obeyed (no particle flow):

$$\frac{T}{\Delta T}\frac{\Delta\mu}{\mu - \varepsilon_r} = 1 \Leftrightarrow \varepsilon_r = \frac{\mu_L T_R - \mu_R T_L}{T_R - T_L} \Leftrightarrow f_L = f_R$$

The energy ε_S fulfills the condition $f_L(\varepsilon_S) = f_R(\varepsilon_S)$, where $f_{R/L}(\varepsilon) = 1/\{1 + \exp[(\varepsilon - \mu_{R/L})/kT_{R/L}]\}$ are the Fermi-Dirac distribution functions in R and L, respectively, shown in Fig. 1(d) for $T_R > T_L$ and $V > 0$. For $\varepsilon > \varepsilon_S$, the probability of finding an electron in reservoir R is higher than in L. Electrons can thus increase the system entropy by moving from R to L, following the temperature gradient. Electrons in the range $\varepsilon < \varepsilon_S$ can increase entropy by following the electrochemical potential gradient from L to R. For $\varepsilon = \varepsilon_S$, where the probability for finding an electron is the same on both sides, the two driving forces cancel. One may say that at this particular energy the two reservoirs behave as if they were in thermal equilibrium with each other. If the two reservoirs were connected via an ideal energy filter that was transparent for electrons at ε_S and at no other energy, no time-averaged particle or heat current would occur spontaneously. The warm bath would not cool, and the voltage would drive no current.

Humphrey et al. PRL 89 116801 (2002)

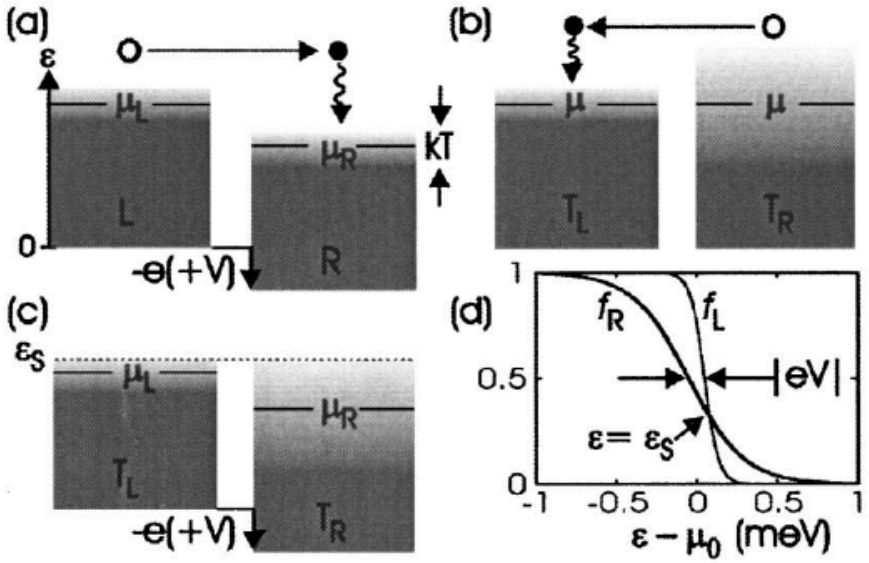

FIG. 1. Electron transfer between reservoirs: (a) in the presence of a difference in electrochemical potentials, (b) in the presence of a temperature difference, and (c) in the presence of both. (d) The Fermi-Dirac distributions in the energy range around $\mu_0 = 0.5(\mu_L + \mu_R)$ for $T_R = 2$ K, $T_L = 0.5$ K, and $V = 0.1$ mV.

Efficiency comparison between Quantum Dot and 1D wire/waveguide

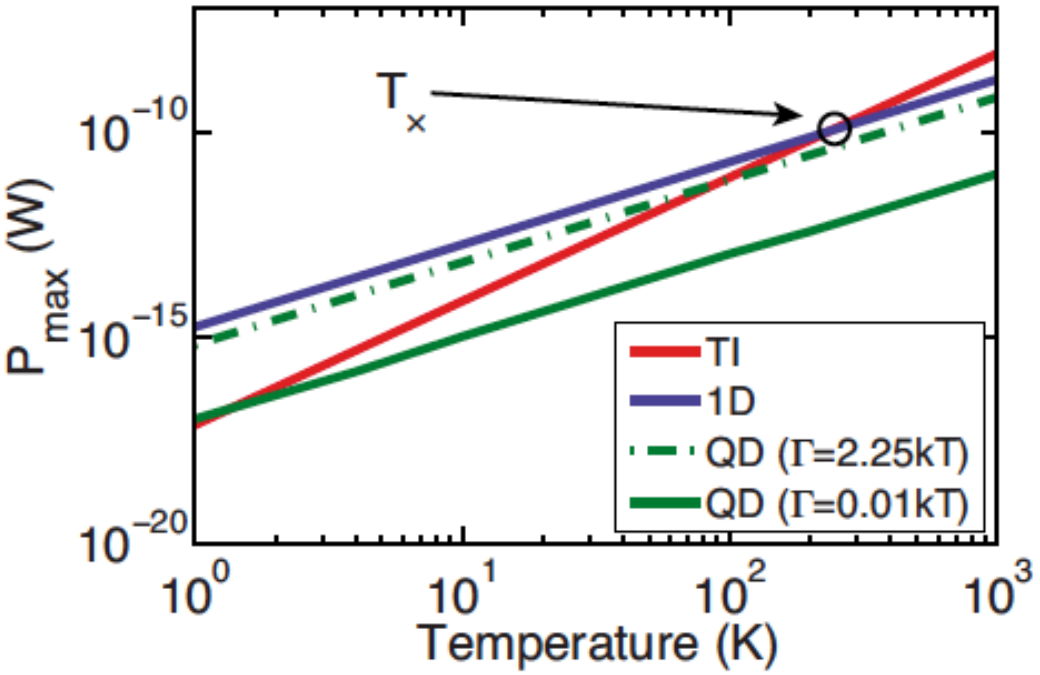

A 1D waveguide filters out unwanted backflow

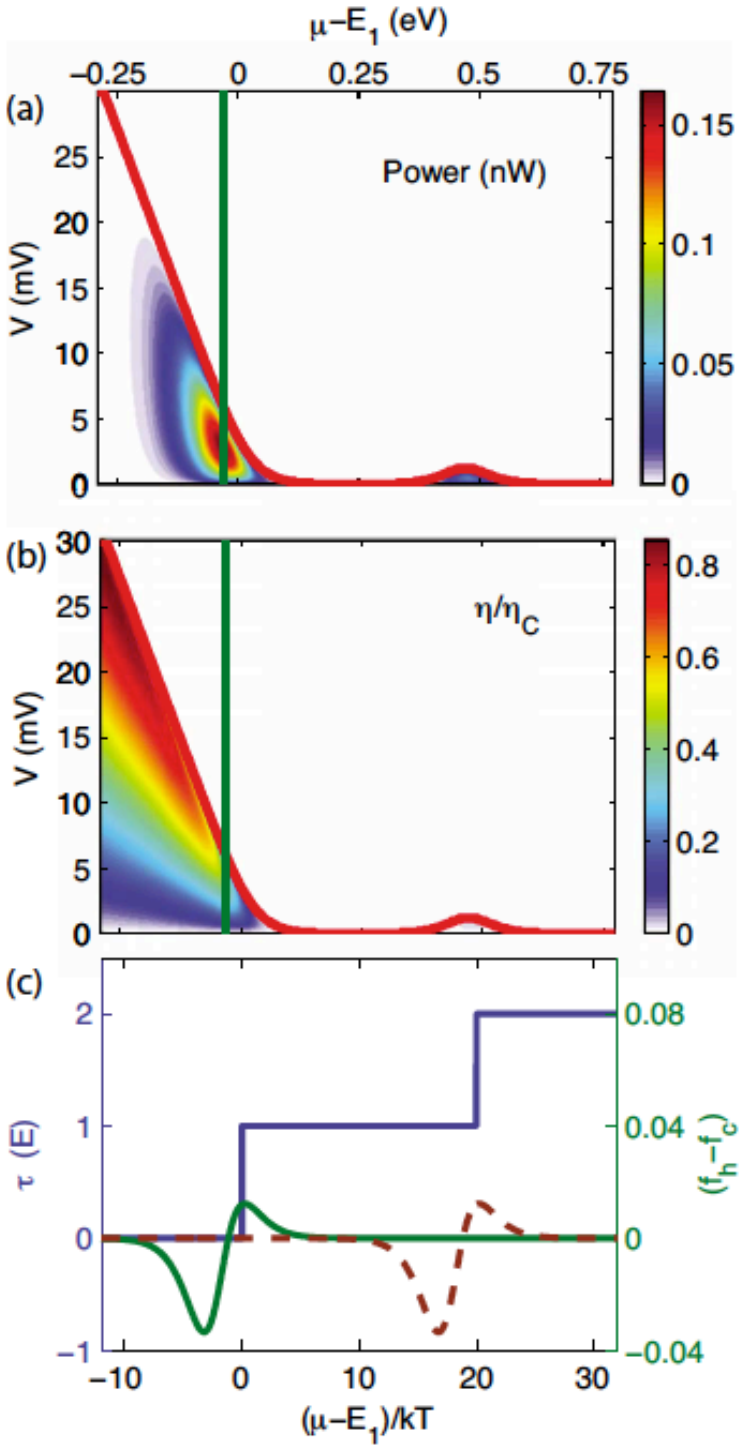

Resonant levels in bulk materials:
band-structure engineering

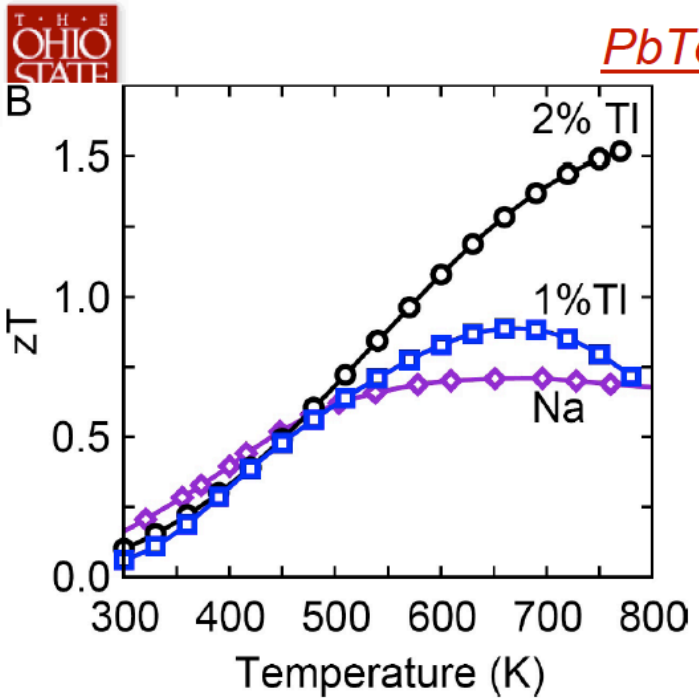

PbTe:Tl doubles zT

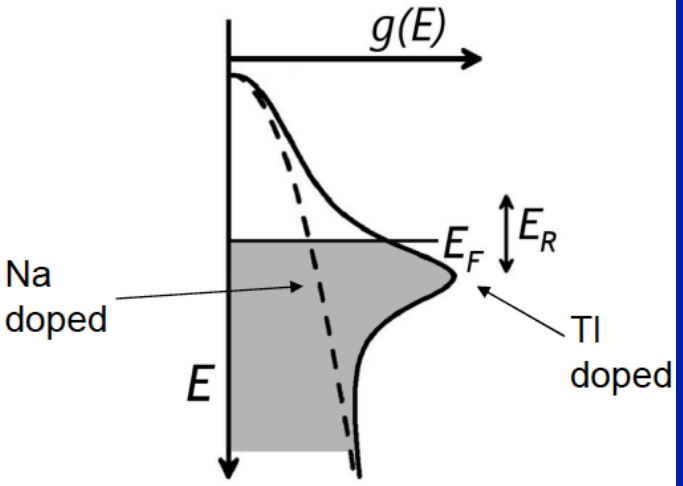

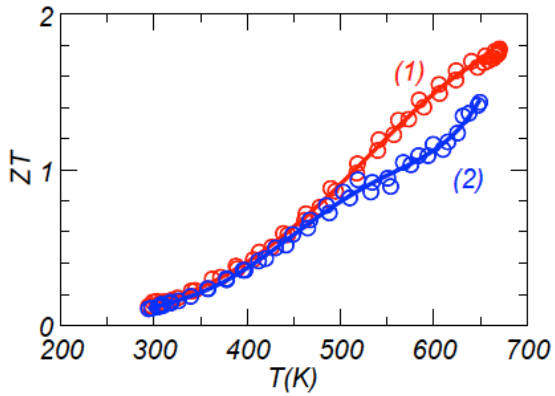

Heremans et al, Science 321 554 2008

8

http://www1.eere.energy.gov/vehiclesandfuels/pdfs/thermoelectrics_app_2009/wednesday/heremans.pdf

Hicks-Dresselhaus: Quantum Wells and Quantum Wires

Hicks and Dresselhaus, 1993; Figs from Heremans and Dresselhaus, Handbook. Thermo. 1998

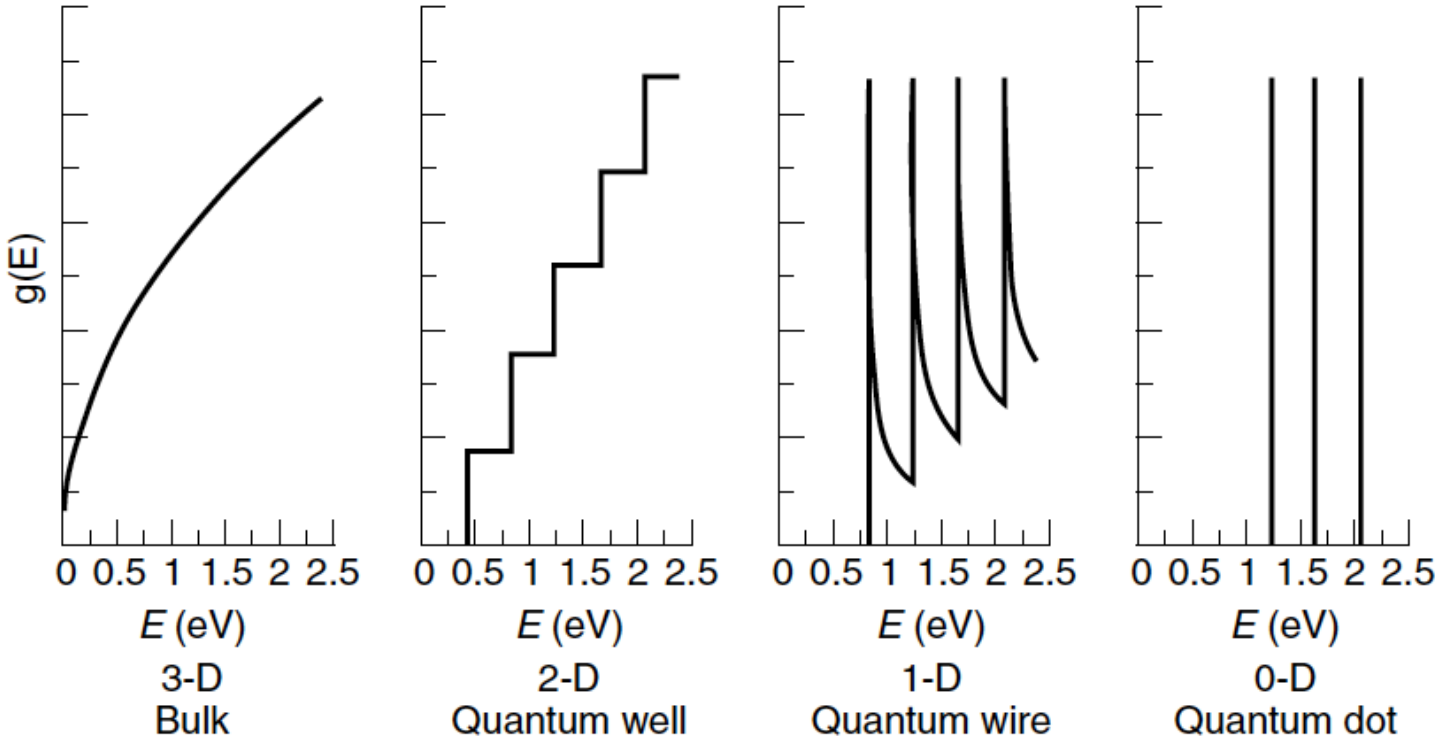

FIGURE 27.1 Electronic density of states $g(E)$ as a function of carrier energy E, for semiconductors of different dimensionality: (a) a bulk three-dimensional (3-D) crystal; (b) a 2-D crystal, or quntum well; (c) a 1-D crystal or quantum wire; (4) a 0-D crystal or quantum dot (see Table 27.1).

Semiconductor
(e.g. Bi2Te3):
3D bulk
2D Quantum well
1D Quantum Wire

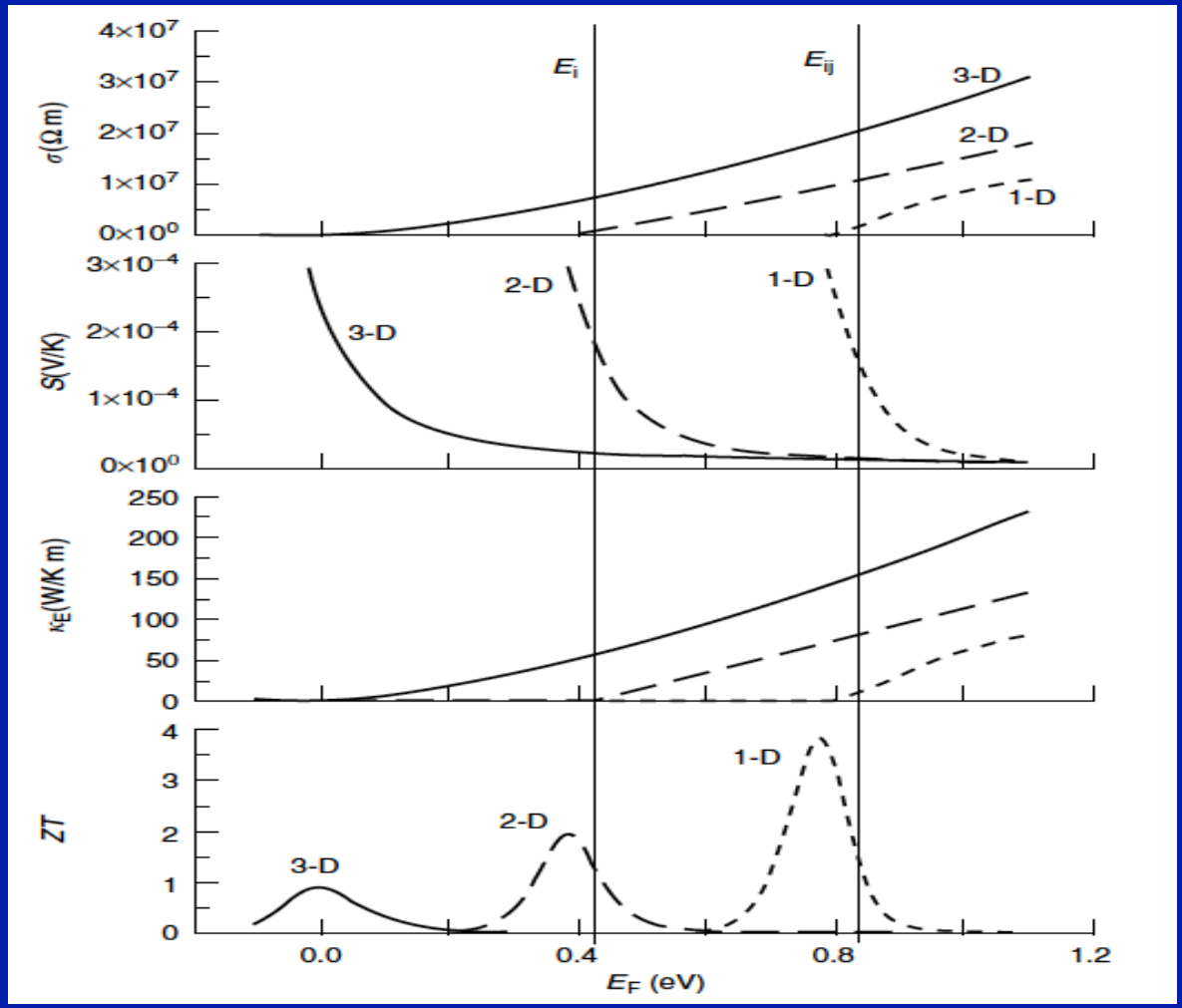

FIGURE 27.2 The transport properties for 3-D (full line), 2-D (long dashes), and 1-D (short dashes) solids as a function of the Fermi energy. The calculations are made at 300 K, and assume an isotropic Fermi surface with $m^* = 0.1m_0$. The thickness of the quantum well and the diameter of the quantum wire are $d = 3$ nm. The value of the first size-quantized subband edge, E_i for 2-D systems and $E_{i,j}$ for a 1-D system, are shown. The Fermi energy in each system has to be chosen by doping to maximize the value of ZT, and the location is different for the different dimensionalities. For the calcualtions of ZT, a constant $\kappa_L = 1.5$ W/m K was used. The maximum achievable ZT is improved as the dimensionality of the system is decreased.

- Nanostructured Materials:
- Increase of ZT from electronic origin demonstrated in Bi nanowires
- Has proven to be an efficient way at reducing the phonon contribution to thermal conductivity !
- Possible Limitations:
- Increase of scattering, especially inelastic

Disentangling band-structure and energy-exchange: 3-terminal devices

Control of inelastic processes

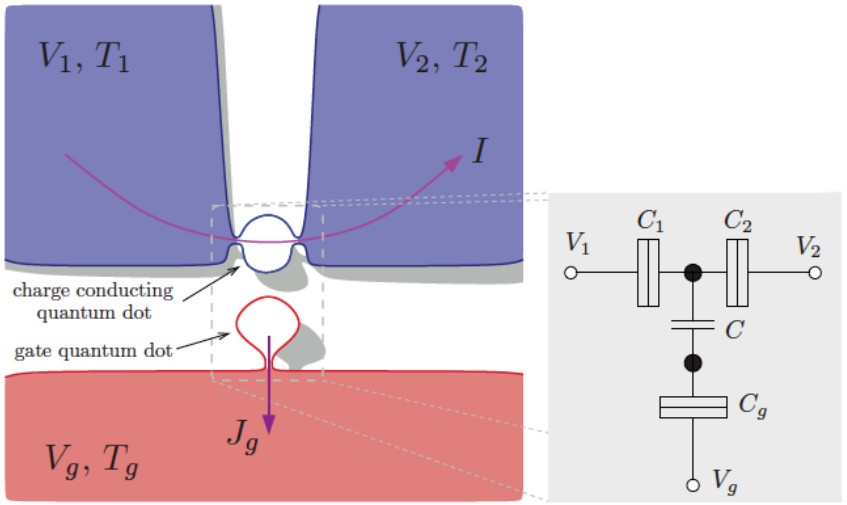

FIG. 1. (Color online) Energy to current converter. The conductor, a quantum dot open to transport between two fermionic reservoirs at voltages V_1 and V_2 and temperatures T_1 and T_2, is coupled capacitively to a second dot which acts as a fluctuating gate coupled to a reservoir at voltage V_g and temperature T_g. Here we discuss the case $T_1 = T_2 = T_s$.

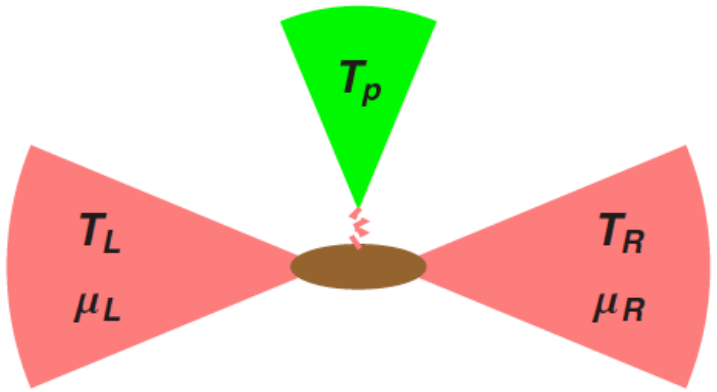

FIG. 1. (Color online) A three-terminal system, modeled by a resonant level attached to two electronic reservoirs, having different chemical potentials and temperatures $\mu_{L,R}$ and $T_{L,R}$, respectively. An electron residing on the level interacts with its vibrational modes. The population of these phonons can be determined by the transport electrons (a "floating molecule") or by a coupling to a phonon source kept at temperature T_P.

two decades ago. Why then, is the market not flooded with new high *ZT* materials? There seem to be two dominant reasons. First, although some new materials with improved *ZT* (for example, nanostructured PbTe, SiGe, skutterudites and Si wire arrays) appear to be entering the market, progress is slow, but not far off the 10 to 15 years typical of commercializing university research results. Possibly, some delay is attributable to the added time associated with initiating government funding at the onset, and the time required to develop fabrication methods to produce thermoelectric material systems that conformed to the theoretical models. Second,

conformed to the theoretical models. Second, the initial concepts were best expressed in thin-film and quantum wire or quantum dot structures using molecular-layering processes. Commercially viable materials are typically 300 μm to several millimetres thick to match electrical and thermal power impedances of the thermoelectric devices to those of external components. Scaling material thickness has proved difficult and has presented technical and cost challenges. The solution is to create self-organizing monolithic structures that conform to the theoretical models, and, in some cases, to adapt semiconductor processing technology to form the needed nanoscale structures. Scaling of high-*ZT* materials is in progress.

Scanning Thermoelectric Microscope

Lyeo et al. Science 303, 817 (2004)

Fig. 2. Measured thermoelectric voltage (circles) and calculated S multiplied by 22 K (line) across a GaAs p-n junction as a function of distance (x). The sample was heated 30 K above the tip (room) temperature. Because of the temperature rise in the tip and in a depletion zone within the nonuniform temperature zone, the value of 22 K yields a better agreement than 30 K between the measurement and the calculation. Inset: STM image of the junction (filled state with a sample bias of –2 V). The bright strip is p-doped with Be at 9×10^{18} cm^{-3}, and the dark strip is n-doped with Si at 1.1×10^{19} cm^{-3}. The dashed line is 150 nm, corresponding to the line where voltage profile is measured.